*Transactions*, SMiRT-24
BEXCO, Busan, Korea - August 20-25, 2017
Division III

# AIRCRAFT IMPACT ON BASE-ISOLATED NUCLEAR POWER PLANT BUILDINGS

**Manish Kumar[1] and Andrew Whittaker[2]**

[1]Assistant Professor, Department of Civil Engineering, Indian Institute of Technology Bombay, India
[2]Professor and MCEER Director, Department of Civil, Structural and Environmental Engineering, University at Buffalo, USA

## ABSTRACT

The United States Nuclear Regulatory Commission (USNRC) defines the impact of large commercial aircraft on a nuclear power plant (NPP) building as a beyond-design basis event. A plant-specific assessment of aircraft impact is required for new reactors.

Seismic isolation is being considered for application to new large light water, small modular and advanced reactors to withstand the effects of extreme earthquakes. This paper investigates the effect of impact of a large commercial aircraft on base-isolated, large light water NPPs. A finite element model of the testbed NPP is analyzed for design basis shaking and aircraft impact. Spectral demands on structures, systems and components inside containment are compared for a) design basis shaking of the conventionally constructed testbed, b) design basis shaking of the base-isolated testbed, and c) aircraft impact loading of the base-isolated testbed. The effects of isolation-system parameters and soil-structure-interaction (SSI) on the earthquake- and impact-related spectral demands are investigated. Elastic material behavior is assumed for the superstructure and the soil, and nonlinear hysteretic behavior is assumed for the lead rubber bearings in the isolation system.

For a given aircraft impact, the installation of seismic isolators increases in-structure spectral demands on containment internal structures, systems and components with respect to the fixed-base condition. In-structure spectral demands due to aircraft impact in a base-isolated NPP are not sensitive to the secant period and/or characteristic strength of an isolation system. The effect of soil-structure interaction on the impact response is large for the fixed-base NPP but relatively small for the base-isolated NPP.

## INTRODUCTION

Seismic isolation using low damping rubber, lead–rubber (LR), and Friction Pendulum™ bearings is a viable strategy for mitigating the effects of extreme earthquake shaking on safety-related nuclear structures. A study supported by the United States Nuclear Regulatory Commission (USNRC) investigated the effect of design and beyond design earthquake shaking on a nuclear power plant (NPP) (e.g., Kumar *et al.* (2015a), Kumar *et al.* (2015b), Kumar *et al.* (2015c), Kumar *et al.* (2014)). The effect of aircraft impact on base-isolated nuclear power plant is investigated here as part of the on-going study. The USNRC defines the impact of large commercial aircraft on a NPP as a beyond-design basis event. A plant-specific assessment of aircraft impact is required per 10 CFR Part 50 (NRC, 1998a) and Part 52 (NRC, 1998b) for new reactors.

Aircraft impact on nuclear structures is not a new topic. Much of initial research was performed by Riera (1968), who proposed a methodology to obtain the load history of aircraft impact on a NPP, also known widely as a Riera loading function. Riera (1980) reported that peak values of in-structure spectral accelerations associated with aircraft impact are expected to be in the range of 8 to 40 Hz, and that the maximum values exceed those due to design basis earthquake shaking (as characterized at that time) at frequencies greater than 10 Hz. The values of in-structure spectral acceleration at higher frequencies are also very sensitive to the numerical techniques (e.g., integrators, damping) employed to calculate response. The artificially sharp corners on the load-history functions introduce high frequency noise. Local nonlinear responses will filter and modify the loadings on the internal structures, components and systems. Andonov *et al.* (2009) reported that enveloping the Riera functions for a given aircraft of different fuel weight and impact velocities does not necessarily provide conservative estimates of in-structure floor spectra.

Kulak and Yoo (2003) analyzed a base-isolated NPP impacted by aircraft but used a SDOF representation of the reactor building and a simplified Riera load function, without consideration of the location of the impact or the mechanical properties of the isolation system. Keldrauk *et al.* (2011) performed parametric analysis with varying isolation period and mass of the superstructure to estimate the response of base-isolated NPP subject to aircraft impact. They concluded that acceleration response is not sensitive to the isolation period but increases when superstructure mass is reduced. The authors assumed linear elastic isolators with 10% damping and modeled the NPP as a three-story shear structure for their calculations.

The limitations of previous research are addressed here and conclusions drawn previously are revisited. A finite element (FE) model of an archetype NPP is used here to investigate the impact of a large commercial aircraft on base-isolated NPPs, considering the effects of isolator properties, location of impact and soil-structure interaction.

## REACTOR MODEL

A FE model of the representative NPP described in Orr (2003) was created in LS-DYNA (LSTC, 2012). The NPP consists of an Auxiliary Building (AB), the Concrete Containment Vessel (CCV), and the Containment Internal Structure (CIS), all sharing a common basemat. The CIS is joined only to the basemat. The AB and CCV are modeled using shell elements, and the CIS and basemat are modelled using solid elements. Linear elastic properties for concrete and steel materials were used. The total mass of the NPP, including the basemat, is 155,000 tons. The dimensions and sectional views of the NPP as well as the locations at which responses are monitored and reported in this paper are shown in Figure 1. Modal properties of the NPP are presented in Figure 2. The first two horizontal modes (Modes 1 and 2) are vibration of the AB and the CCV in the horizontal directions. The next two horizontal modes (Modes 9 and 10) are vibration of the CIS. Mode 16 is vertical vibration of the AB.

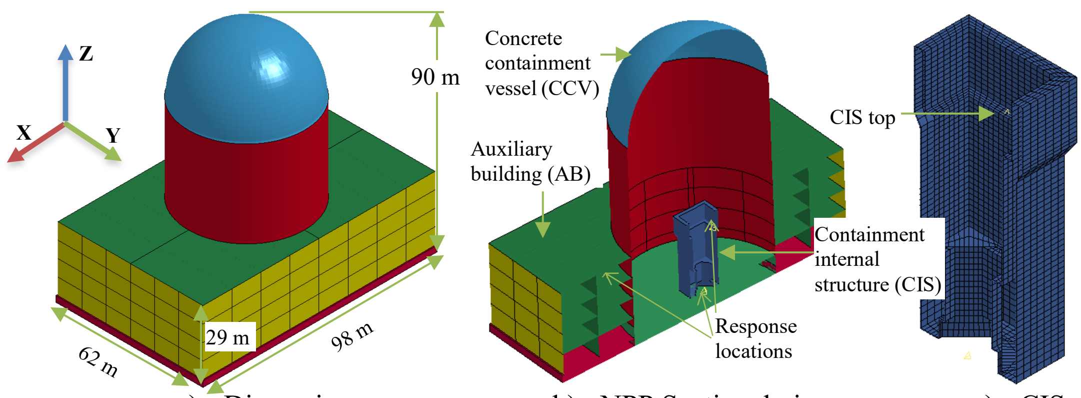


a) Dimension b) NPP Sectional view c) CIS

Figure 1: Finite element model of the archetype NPP

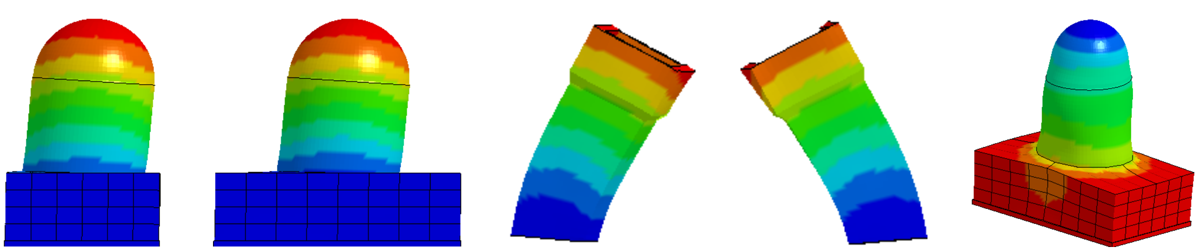

*f* = 3.47 Hz a) Mode 1 | *f* = 3.62 Hz b) Mode 2 | *f* = 7.02 c) Mode 9 | *f* = 7.02 d) Mode 10 | *f* = 8.96 Hz e) Mode 16

Figure 2: Modal responses of the model of the NPP

## ISOLATION SYSTEM

The NPP is isolated on a common basemat slab using a symmetrical layout of 273 LR bearings. The dimensions of the reinforced concrete basemat are 98 m × 62m × 2.5m. LS-DYNA provides a direct option to model elastomeric bearings through a material model *MAT_SEISMIC_ISOLATOR. Behavior in the two horizontal (shear) directions is based on the model proposed by Park *et al.* (1986) and extended for seismic isolators by Nagarajaiah *et al.* (1989). The vertical stiffness for all types of isolators is linear elastic, with the option to provide different values in compression and tension. Additional details on modeling a seismic isolator using *MAT_SEISMIC_ISOLATOR is provided in LS-DYNA User's Manual (LSTC, 2012). The advanced model of the lead-rubber bearing per Kumar et al. (2014) was not required for these analyses because the horizontal deformation demands were small, as described later.

The geometric and mechanical properties of the LR bearings used for the analysis are summarized in Table 1. The procedure to obtain these properties is described in Kumar *et al.* (2015c). Most of the analyses were performed with the isolation system with a ratio of characteristic strength to supported weight, $Q_d / W$ , equal to 0.12.

Table 1. Geometrical and mechanical properties of elastomeric bearings

| Property | Notations (units) | $T = 2$ s | $T = 3$ s | |
|---|---|---|---|---|
| | | $Q_d/W = 0.12$ | $Q_d/W = 0.12$ | $Q_d/W = 0.06$ |
| Single rubber layer thickness | $t_r$ (mm) | 10 | 10 | 10 |
| Number of rubber layers | $n$ | 31 | 31 | 31 |
| Steel shim thickness | $t_s$ (mm) | 4.75 | 4.75 | 4.76 |
| Outer diameter | $D_o$ (mm) | 1548 | 1548 | 1532 |
| Inner/lead core diameter | $D_i$ (mm) | 317 | 317 | 224 |
| Rubber cover thickness | $t_c$ (mm) | 25 | 25 | 25 |
| Shear modulus | $G$ (MPa) | 0.94 | 0.42 | 0.42 |
| Bulk modulus of rubber | $K_{bulk}$ (MPa) | 2000 | 2000 | 2000 |
| Yield stress of lead | $\sigma_L$ (MPa) | 8.5 | 8.5 | 8.5 |
| Horizontal yield displacement | $u_y$ (mm) | 21 | 21 | 21 |
| Static pressure due to gravity loads | $p_{static}$ (MPa) | 3.0 | 3.0 | 3.0 |

## DAMPING

A Rayleigh damping formulation was used for the superstructure and the isolators. The superstructure was assigned a mass damping of 4% based on its first horizontal frequency and a damping of 4% using a stiffness damping formulation defined in LS-DYNA that uniformly damps all the high frequency modes (LSTC, 2016). Isolators were assigned a mass damping of 2% based on the horizontal isolation frequency and 2% stiffness damping. The mass and stiffness damping assigned to the isolators supplemented the hysteretic damping provided by the LR bearings due to energy dissipation in the lead cores. Additional information on modeling damping is available in Kumar and Whittaker (2018).

## ANALYSIS CASES

Fixed and base-isolated models of NPPs were analyzed for aircraft and design basis earthquake loadings. The effects on response of isolation period and normalized characteristic strength were investigated. Two locations of impact were considered. The effects of SSI on the predicted response of the NPPs to aircraft impact were also characterized.

Results of the seismic and impact analysis are reported here for the X direction only: the direction of aircraft impact, as shown in Figure 1. Results of the analyses in the Z direction are substantially influenced by the treatment of damping in the vertical direction, which is beyond the scope of this paper. Kumar and Whittaker (2018) present complete results of the seismic and aircraft impact analyses.

## SEISMIC RESPONSE-HISTORY ANALYSIS

The response-history analyses of the NPPs were performed using sets of three-component ground motions selected and then spectrally matched to be consistent with uniform hazard response spectra (UHRS) for design-basis earthquake shaking at the site of the Diablo Canyon Nuclear Generating Station. The UHRS were calculated for a return period of 10,000 years and 5% damping. The response spectra of the ground motion in the two horizontal and the vertical direction is shown in Figure 3. The in-structure (floor) response spectra at the center of the basemat, top of the CIS and 3rd floor of the auxiliary building in the fixed-base and base-isolated NPPs, are presented in Figure 4 through Figure 6, respectively (See Figure 1 for the monitoring locations.) Base isolation of the NPP substantially reduces its seismic response in the horizontal direction. Additional results and discussion are presented in Kumar and Whittaker (2018).

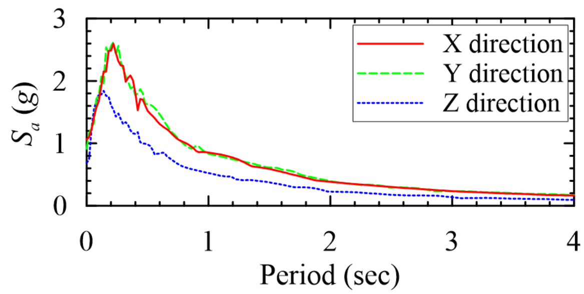


Figure 3: Acceleration response spectra of ground motions

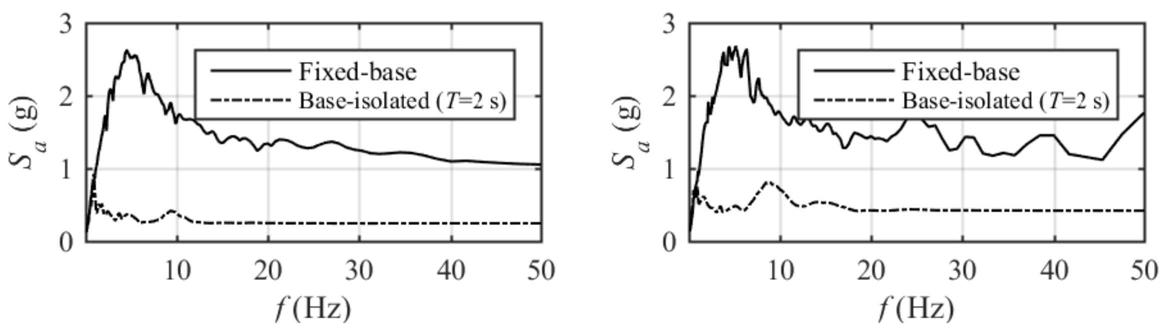


a) X direction b) Y direction

Figure 4: In-structure response spectra at the center of basemat: design-basis earthquake loading

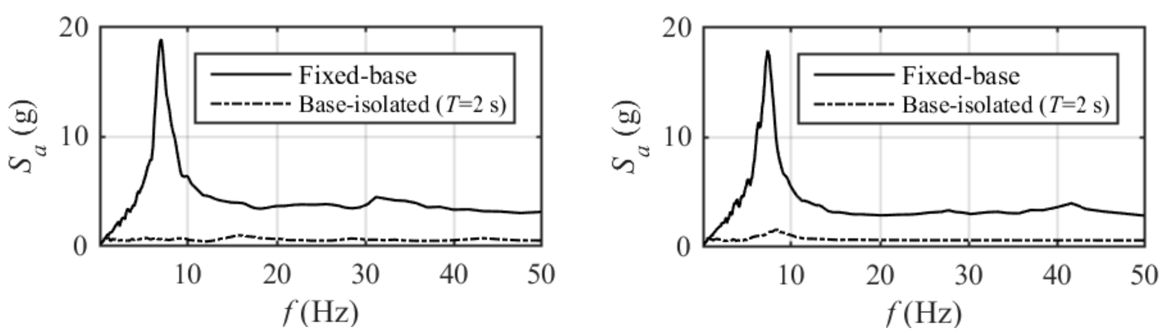


a) X direction b) Y direction

Figure 5: In-structure response spectra at the top of the CIS: design-basis earthquake loading

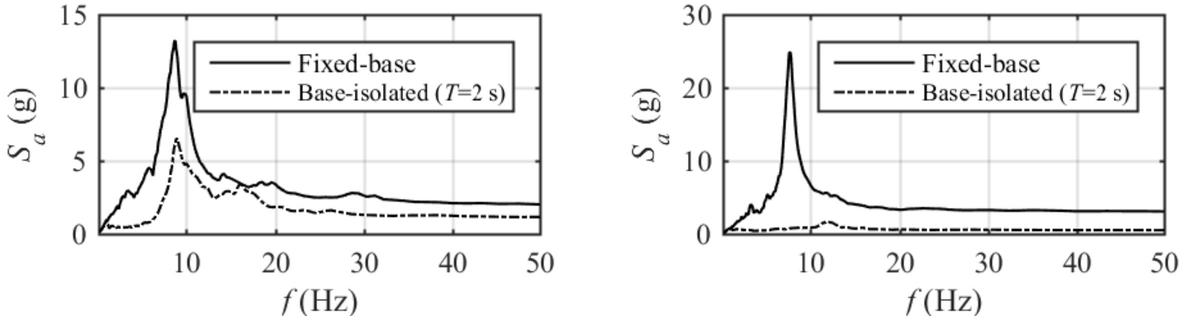


a) X direction b) Y direction

Figure 6: In-structure response spectra at the 3rd floor of the auxiliary building: design-basis earthquake loading

## AIRCRAFT IMPACT ANALYSIS

Riera (1968) proposed a force history for the normal impact of an aircraft on a rigid reflecting surface:

$$F_x(t) = P_c + \rho v^2 \tag{1}$$

where $P_c$ is the axial buckling or crushing strength, $\rho$ is the mass density, and $v$ is the impact velocity. Interaction of the structure and the aircraft is not considered. The accuracy of the load history obtained using Equation (1) depends on the validity of two assumptions: 1) the target is rigid and the orientation of the impact is such that the fuselage buckles axially, and 2) the mass distribution and fuselage crushing strength of the aircraft. For oblique impact and non-rigid targets, the force obtained using Equation (1) is conservative (Riera, 1980).

Riera load histories have been developed for a number of commercial aircraft. The key parameters are the mass density and crushing strength of the aircraft along its length. The load history is applied over an assumed area of impact. The area over which the load is applied can be assumed equal to the average cross-sectional area of fuselage. The impact of the Boeing 747-400 is considered here using the loading history of Iliev *et al.* (2011). The impact velocity is assumed to be 120 *m*/*s*. An impact area of 100 $m^2$ is used, which is the average cross-section area of the fuselage and the wing, as shown in Figure 7.

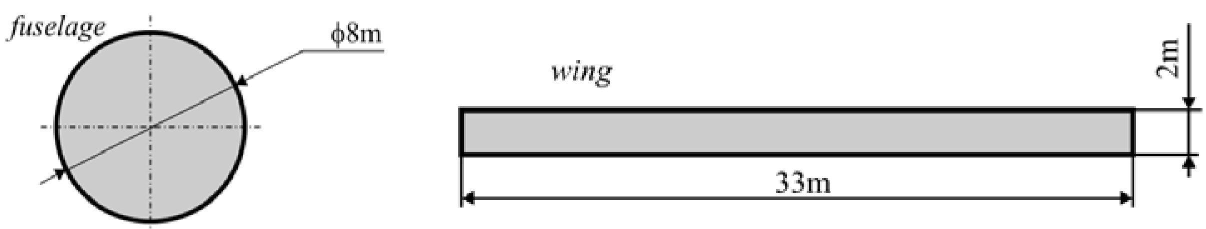


Figure 7: Effective area of impact for the Boeing 747-400 aircraft (Iliev *et al.*, 2011)

The Riera function for B747-400 at an impact velocity of 120 *m*/*s* is presented in Figure 8. Two impact locations were considered, as shown in Figure 9: 1) Location 1, 71 m above basemat, at the mid-height of the dome of the containment vessel, and 2) Location 2, 48 m above basemat, at the 3/4 height of the cylindrical part of the containment vessel, above the roof of auxiliary building. The impact load was applied in LS-DYNA as a pressure vector perpendicular to individual shell elements.

The in-structure response spectra in the direction of loading (X) for impact at Location 1, in the fixed-base and base-isolated NPPs are presented in Figure 10. The energy of the impact is transferred through the CCV and the attached auxiliary building to the ground, which results in high accelerations in these components of the structure. Small floor accelerations are calculated for the basemat of the fixed-base NPP and in the containment internal structure because of the assumed boundary conditions. In the isolated

NPPs, the entire building is set in motion by the impact, generating high spectral accelerations on the basemat and in the containment internal structure. The spectral accelerations in the auxiliary building, at the location chosen to report results, are not changed substantially by the installation of the isolation system. The period of the isolation system has no significant effect on the in-structure response spectra.

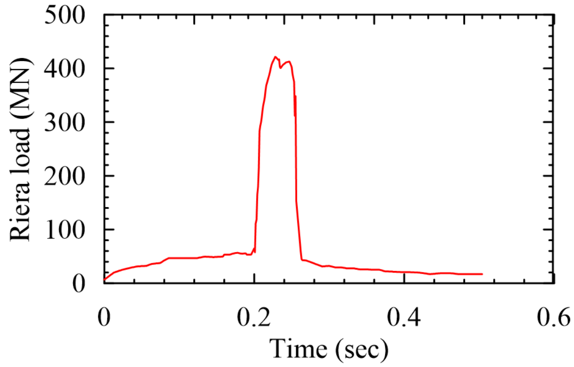


Figure 8: Riera function for a B747-400

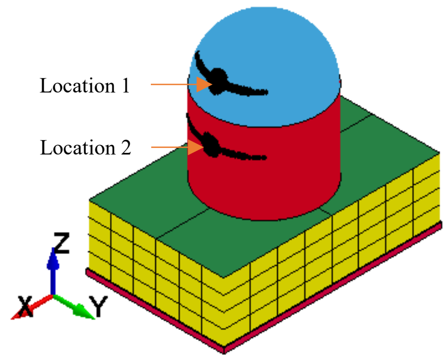


Figure 9: Assumed locations of aircraft impact

The in-structure response spectra in the base-isolated NPPs for aircraft impact at Location 1 and design basis earthquake shaking are presented in Figure 11. The spectral accelerations due to aircraft impact are greater than those associated with design basis earthquake shaking at moderate and high frequencies.

The effect of location of impact on the response of the NPP is investigated next. In-structure response spectra for the two locations of impact are presented in Figure 12. The spectral demands at high frequencies are smaller for the lower impact (i.e., Location 2).

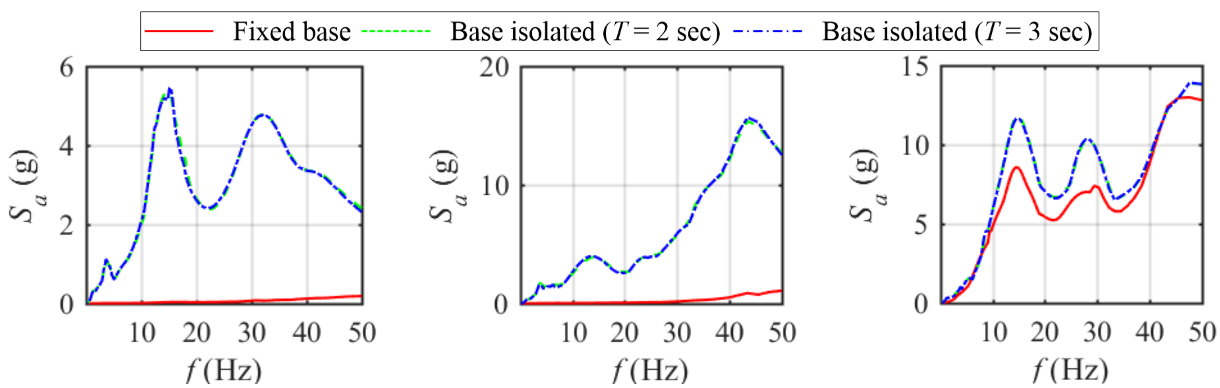


a) Basemat b) Containment internal structure c) Auxiliary building

Figure 10: In-structure response spectra (X direction) due to aircraft impact at Location 1

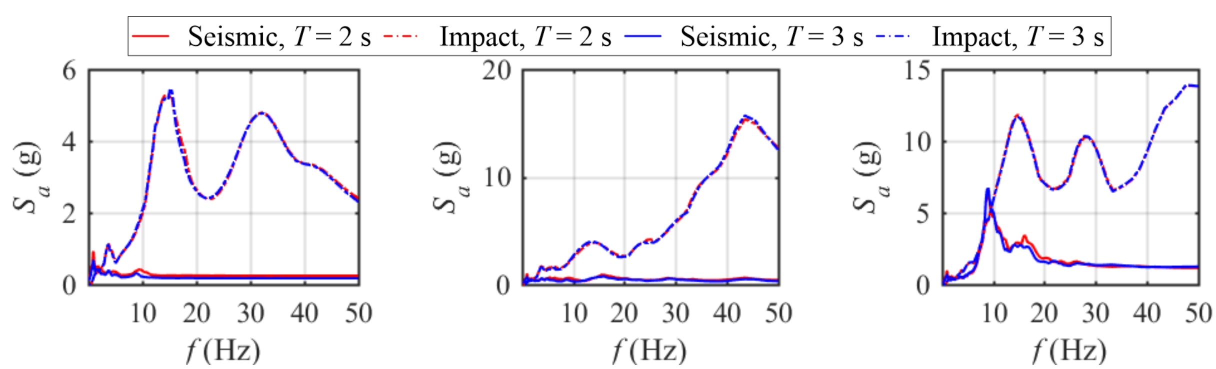


a) Basemat b) Containment internal structure c) Auxiliary building

Figure 11: In-structure response spectra (X direction) in the base-isolated nuclear power plants

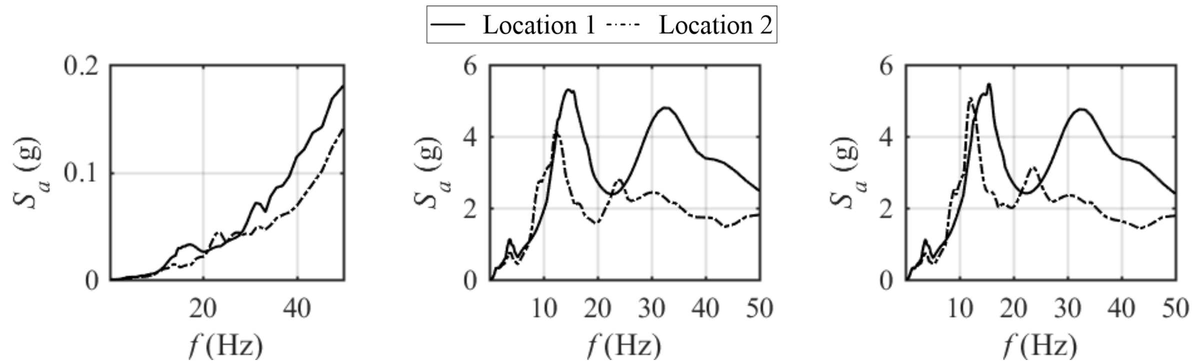


a) Fixed-base b) Base-isolated ($T$ = 2 s) c) Base-isolated ($T$ = 3 s)

Figure 12: In-structure response spectra (X direction) at the basemat of the NPP associated with aircraft impact

The response of the fixed-base NPP due to aircraft impact is benchmarked against the seismic response of the corresponding base-isolated NPP in Figure 13. The spectral demands due to aircraft impact on the fixed-based NPP are greater than those associated with design basis earthquake shaking for the base-isolated NPPs at frequencies less than 10 Hz. The horizontal responses of one of the isolators for aircraft impact at Location 1 and design basis earthquake shaking are presented in Figure 14.

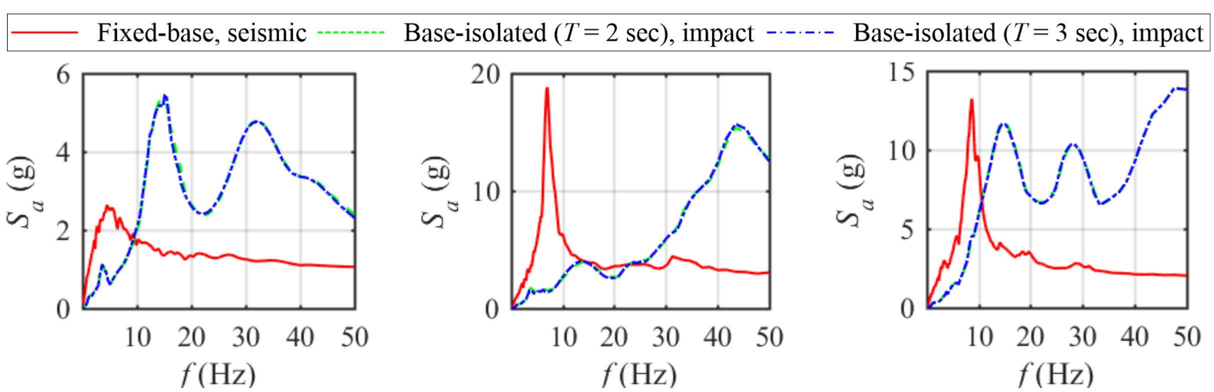


a) Basemat b) Containment internal structure c) Auxiliary building

Figure 13: In-structure response spectra (X direction) in the fixed-base and base-isolated NPPs

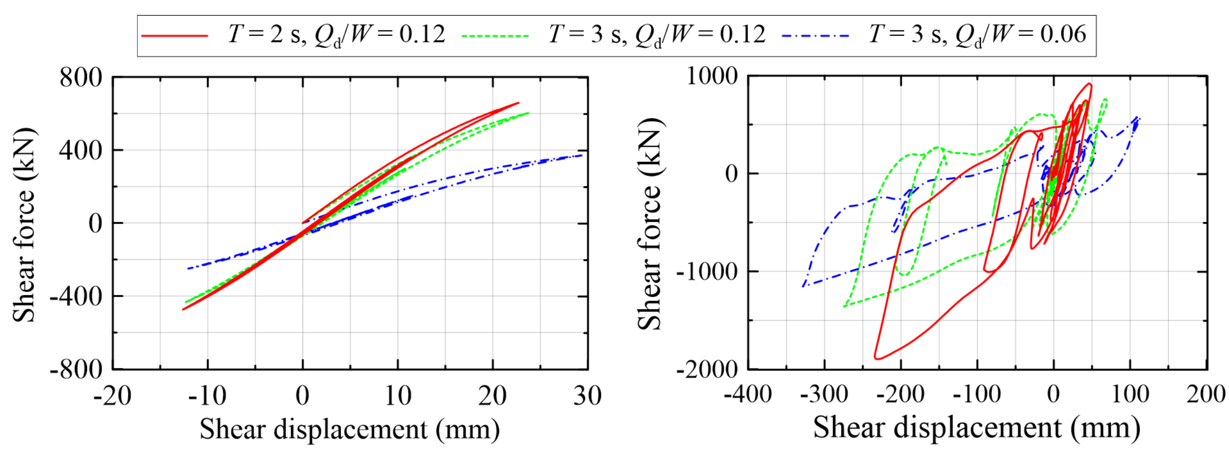


a) Aircraft impact b) Earthquake excitation

Figure 14: Horizontal response of the isolator at the center of the basemat of the base-isolated NPPs

The isolator response due to aircraft impact is essentially elastic and no energy dissipation is observed. This is primarily due to relatively large strength of the LR isolation system in the horizontal direction and the large mass of the isolated superstructure. The effect of isolation-system strength on the aircraft impact response was investigated by considering an isolation system with a secant period of 3 seconds and a ratio of strength to supported weight of 0.06 (*T*3*Q*6): one half of that considered previously. The properties of the LR bearings in this isolation system ($T = 3$ sec, $Q_d/W = 0.06$) are presented in Table 1. The choice of characteristic strength, in the practical range considered here, has no meaningful effect on either the acceleration or the displacement response of this base-isolated NPP due to aircraft impact.

## SOIL-STRUCTURE INTERACTION

There are different strategies to include soil-structure interaction in LSDYNA. The soil domain was modeled here using a perfectly matched layer (PML). A PML layer is placed next to the elastic soil medium to absorb all the waves travelling through without any reflection from the domain boundary. The absorbing boundary condition using a PML has recently been implemented in LS-DYNA by Basu (2009).

The elastic properties of the soil were back-calculated assuming a shear wave velocity of 760 m/sec, which corresponds to the boundary of site class B and C per ASCE 7-10 (ASCE, 2010). Poisson's ratio and the density of the soil were assumed to be 0.3 and 2400 kg/m$^3$, respectively. A representative damping value of 5% was assigned to the elastic soil to account for viscous and radiation damping.

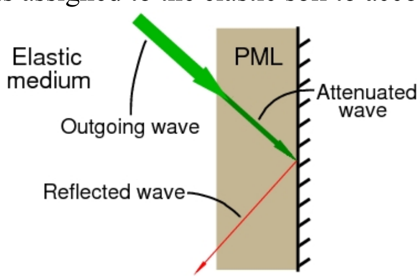


Figure 15: Modeling of the absorbing soil boundary using perfectly matched layer (LSTC, 2017)

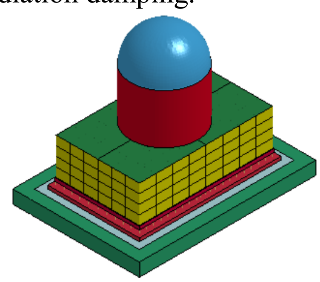

Figure 16: The finite element model of a base-isolated NPP including SSI effects

The in-structure response of the fixed and base-isolated ($T = 2$ sec) NPP due to aircraft impact at Location 1, with and without SSI effects, are presented in Figure 17 and Figure 18, respectively. Soil-structure interaction dramatically increases in-structure spectral demands at the basemat and on the CIS of the non-isolated NPP because the basemat is put into motion by the impact. The effects of SSI on in-structure spectra at the monitoring location in the auxiliary building are tiny. Ignoring SSI for aircraft impact analysis will lead to an underestimation of spectral demands at key locations in a NPP.

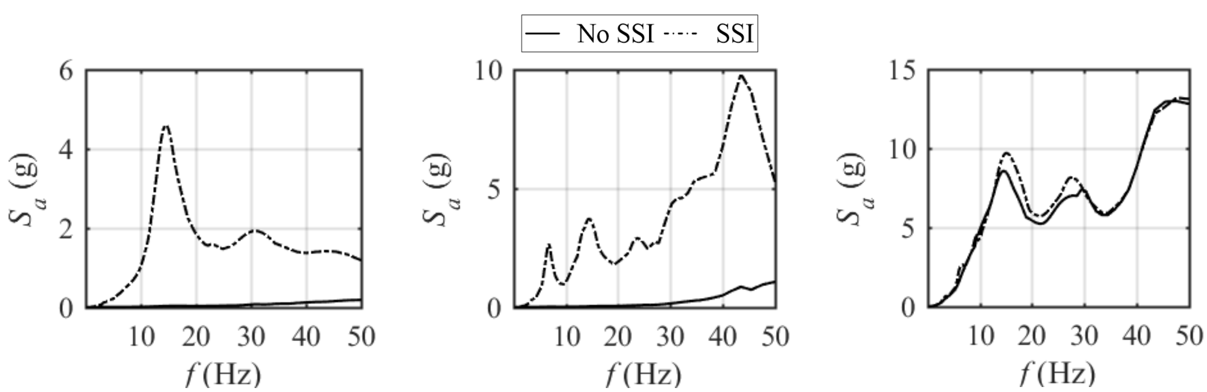


a) Basemat b) Containment internal structure c) Auxiliary building

Figure 17: In-structure response spectra (X) in a non-isolated NPP due to aircraft impact, considering SSI

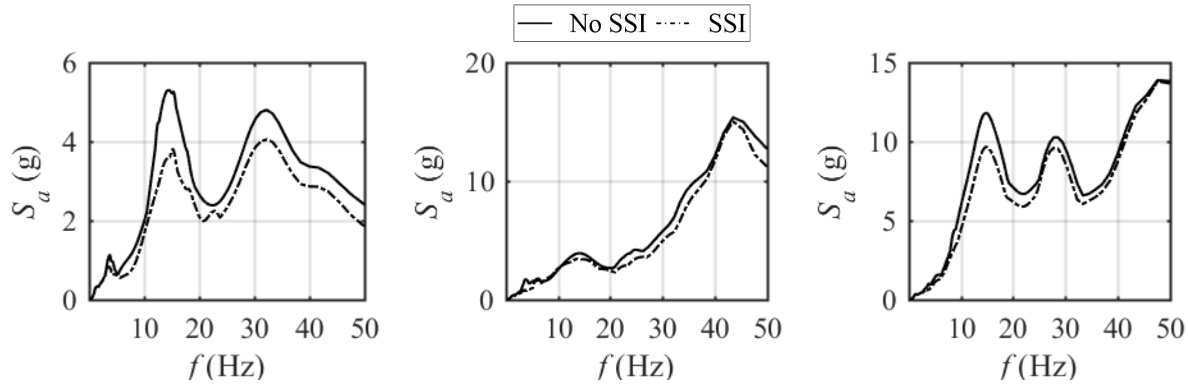


a) Basemat b) Containment internal structure c) Auxiliary building

Figure 18: In-structure response spectra (X) in an isolated NPP due to aircraft impact, considering SSI

## SUMMARY AND CONCLUSIONS

The effects of impact of a large commercial aircraft on archetype conventionally founded and base-isolated NPPs were investigated by FE analysis. A detailed FE model of the NPP was built in LS-DYNA and the impact loading function was obtained using the methodology proposed originally by Riera (1968). Several analysis cases were considered to investigate factors that affect the response of the archetype NPP. The key conclusions, which are somewhat specific to the choice of aircraft, impact velocity, size and mass of the archetype NPP, and the seismic design basis for the NPP, are:

1. In-structure spectral demands due to aircraft impact in a base-isolated NPP will be greater than those in its *fixed-base* counterpart because the isolated basemat is put into motion.
2. The inclusion of a compliant soil domain beneath the NPP will lead to higher in-structure spectral demands than those in the *fixed-base* counterpart because the basemat is put into motion: soil-structure interaction. The effect of soil-structure interaction on the response of the isolated building due to impact is relatively small.
3. The peak floor spectral acceleration in a base-isolated NPP due to aircraft impact is smaller than that due to design basis shaking of the corresponding fixed-base NPP at frequencies less than 10 Hz.
4. In-structure spectral demands due to aircraft impact in a base-isolated NPP are insensitive to the secant period and/or characteristic strength of an isolation system.
5. The response of the isolation system due to impact of a large commercial aircraft is essentially elastic for the NPP of the size and mass considered here. Consequently, damping in an isolator does not significantly affect the response of a NPP due to aircraft impact.

## ACKNOWLEDGEMENTS

Financial support for this research project was provided by the United States Nuclear Regulatory Commission (USNRC) through a grant to MCEER via a contract led by Dr. Robert Budnitz at the Lawrence Berkeley National Laboratory (LBNL). The authors acknowledge the important technical contributions of the Dr. Budnitz, the LBNL review panel, and Dr. Jose Pires of the USNRC to this research project.

## REFERENCES


Andonov, A., Apostolov, K., Stefanov, D., and Kostov, M. (2009). "On the floor response spectra due to aircraft impact." *Proceedings: 20th International Conference on Structural Mechanics in Reactor Technology (SMiRT 20)* Helsinki, Finland.

American Society of Civil Engineers (ASCE). (2010). "Minimum design loads for buildings and other structures." *ASCE/SEI Standard 7-10*, Reston, VA.

Basu, U. (2009). "Explicit finite element perfectly matched layer for transient three-dimensional elastic waves." *International Journal for Numerical Methods in Engineering*, 77(2), 151-176.

Iliev, V., Georgiev, K., and Serbezov, V. (2011). "Assessment of impact load curve of Boeing 747-400." *Machines, Technologies, Materials: International Scientific Journal*, 1(1), 22-25.

Keldrauk, E., Peterson, P. F., and Stojadinovic, B. (2011). "Framework for performance-based evaluation and design of seismic isolation for nuclear energy facility structures." *Proceedings: 21st International Conference on Structural Mechanics in Reactor Technology (SMiRT-21)* New Delhi, India.

Kulak, R. F., and Yoo, B. (2003). "Effects of aircraft impact on a seismically isolated reactor building." *Proceedings: 17th International Conference on Structural Mechanics in Reactor Technology (SMiRT-17)* Prague, Czech Republic.

Kumar, M., Whittaker, A., and Constantinou, M. (2014). "An advanced numerical model of elastomeric seismic isolation bearings." *Earthquake Engineering and Structural Dynamics*, 43(13), 1955-1974.

Kumar, M., Whittaker, A., and Constantinou, M. (2015a). "Seismic isolation of nuclear power plants using elastomeric bearings." Technical Report MCEER-15-0008, University at Buffalo, State University of New York, Buffalo, NY.

Kumar, M., Whittaker, A., and Constantinou, M. (2015b). "Experimental investigation of cavitation in elastomeric seismic isolation bearings." *Engineering Structures*, 101, 290-305.

Kumar, M., Whittaker, A., and Constantinou, M. (2015c). "Response of base-isolated nuclear structures to extreme earthquake shaking." *Nuclear Engineering and Design*, 295, 860–874.

Kumar, M., and Whittaker, A. (2018). "Beyond design basis considerations for base-isolated nuclear power plants." *Report in preparation*, Technical Report MCEER-18-xxxx, University at Buffalo, State University of New York, Buffalo, NY.

Livermore Software Technology Corporation (LSTC) (2012). "LS-DYNA keyword user's manual, volume 2: material models." Livermore, CA.

Livermore Software Technology Corporation (LSTC) (2016). "Damping in LS-DYNA." <http://www.dynasupport.com/howtos/general/damping>. (November 1, 2016).

Livermore Software Technology Corporation (LSTC) (2017). "PML absorbing boundary." <http://www.lstc.com/applications/soil_structure/pml>. (April 1, 2017).

Nagarajaiah, S., Reinhorn, A. M., and Constantinou, M. C. (1989). "Nonlinear dynamic analysis of three-dimensional base-isolated structures (3D-BASIS)." Technical Report NCEER-89-0019, University at Buffalo, State University of New York, Buffalo, NY.

United States Nuclear Regulatory Commission (NRC). (1998a). "Domestic licensing of production and utilization facilities." *10 CFR part 50*, Washington, DC.

United States Nuclear Regulatory Commission (NRC). (1998b). "Licenses, certifications, and approvals for nuclear power plants." *10 CFR part 52*, Washington, DC.

Orr, R. (2003). "AP1000 inputs for 2D SASSI analyses." Westinghouse Electric Company, Cranberry Township, PA.

Park, Y. J., Wen, Y. K., and Ang, A. H. S. (1986). "Random vibration of hysteretic systems under bi-directional ground motions." *Earthquake Engineering and Structural Dynamics*, 14(4), 543-557.

Riera, J. D. (1968). "On the stress analysis of structures subjected to aircraft impact forces." *Nuclear Engineering and Design*, 8(4), 415-426.

Riera, J. D. (1980). "A critical reappraisal of nuclear power plant safety against accidental aircraft impact." *Nuclear Engineering and Design*, 57(1), 193-206.